ISSN 1846-6168 (Print), ISSN 1848-5588 (Online)
https://doi.org/10.31803/tg-20250228210232

Original scientific paper
Received: 2025-02-28, Accepted: 2025-03-17

Technical Evaluation Pre-Dehydration Stage under Off-Solar Duration Equipped with Thermal Backup and Cyclic Fan Operation

Nursiwan, Samsul Arifin, Budhi Muliawan Suyitno, Reza Abdu Rahman*

Abstract: This work assesses off-solar duration (OSD) dehydration using three volumetric air flows (VAF) which operate under continued, long and short intermittency cycles. VAF and fan continuity is proportional to total water removed of the product with a maximum capacity of 47.3%. However, it costs higher energy consumption, which only results in maximum effective level of fan by 142.4%. Operating the fan under short intermittency at medium VAF achieves a higher effectivity up to 342.5%. The water diffusion of seaweed is a complex and time-consuming process, making the designed operation favorable to enhance effective energy consumption. Employing thermal backup reaches equilibrium moisture quickly under continuous cycle. However, it has the lowest energy effectiveness (only 6.9%), while setting the target to achieve critical moisture offers higher value at 22.7% using short-intermittency cycle. It shows OSD offers reliable results to reduce the midday cycle duration and ensure minimum losses rather than open dehydration.

Keywords: efficiency; heat storage; intermittency; seaweed; vaporization

1 INTRODUCTION

Population escalated significantly, requiring tremendous amount of food to sustain human life. The process is directed more sustainably to ensure it gives little impact on the environment. It comes as global goal to achieve responsible consumption and production as part of SDGs. The sector is accompanied by rapid development and technological improvement to harvest more clean energy from renewable sources [1–3]. Food processing has become more complex in modern era to accommodate the high variation and global trend, causing high energy consumption in this sector. Specifically, one good example comes from the postharvest handling of aquaculture product (seaweed). The harvested product is handled for dehydration process to extend the lifetime of product and facilitate the next production step. However, dehydration is an extensive energy process due to high latent heat of vaporization for water, approximately 40 kJ/mol [4]. From local perspective, the coastal region from major country producers demands specific technical consideration, which makes industrial-grade drying equipment commonly not used for local farmers [5]. It results in conventional drying by exposing the product directly to solar radiation, which is easier, requires no additional equipment, and takes no additional processing cost.

Direct dehydration during midday supports clean energy utilization and meets the base criteria for sustainable production. Nevertheless, it leads to different problems, such as product degradation due to direct exposure to dirt. Employing direct dehydration gives additional labor cost and highly depends on solar power, followed by quality drops, which reduces the value of the dried product. Consequently, the process becomes economically unfavorable. Solving the issue is performed using closed greenhouse dehydrator (CGD). It remains harvest solar energy, which contributes in energy mix, and simultaneously performs dehydration process in closed room, reducing soiling factor significantly. Labor costs potentially reduce while the product quality increases, making this approach more economically feasible. The difference in relative humidity and temperature (RH/T) inside the CGD and the outdoor potentially causes natural convection, allowing the air to circulate from outside [6]. For higher rate, forced convection is generally used by forcing air to circulate at designed conditions using fluid machine such fan/blower [7]. The energy for operating the machines can be supplied by various sources such wind and solar energy [8–10]. Thus, the system operates primarily by using renewable source to perform dehydration process.

The main technical problem for utilizing CGD is linked specifically to poor dehydration rate compared to industrial-grade dryers. It is highly associated with low solar intensity per unit area [11], making further modification essential to enhance the CGD capacity. Researcher performed several modifications by equipping the system with solar heat collector (SHC). The work [11] used evacuated tube-SHC, which combined with heat energy material (HEM), allowing the supplied air to reach higher temperature (100 °C) with potential to reduce CO_2 and cost per mass flow (< 1 $/kg). The reliability of the system is enhanced by employing latent HEM to improve the storage capacity and thermodynamic aspect [12-14]. In addition, the HEM was modified through encapsulation to prevent leak, which remains shows desirable performance for heating air up to 82 °C [15]. The ideal combination of SHC-CGD promotes the system to operate maximally and reduce the low dehydration rate. Suitable modification of the combined system reached higher extraction rate of water content with lower energy consumption around 0.34 kg/kWh [16]. Many reports demonstrate that the system (CGD with SHC and HEM) has technical feasibility and better performance than non-combined CGD. However, the process uses fan, which consumes energy and requires additional attention regarding the operation behavior of the unit.

Dehydration of the water content from the product depends not only on heat supply but also on mass transfer. The continued operation flow (COF) of the working fan contributes to high specific energy consumption for the process [17]. Thus, modification of the fan operation is done

by adjusting its cycle. For example, M. Li et al. assessed the intermittent operation (IOF) for infrared dryer to dehydrate jujube, showing the proposed operation model potentially improved the quality of the product [18]. The IOF operation is applicable as well for heat pump dehydrator. Y. Hou et al. conducted detail analysis of IOF operation on dehydration of corn kernels, resulting in positive contribution on all IOF setting compared to COF based on the dehydration rate with maximum value of 19.5% [19]. The study [20] utilized solar-electric technology for onion product and compared COF/IOF operation. It showed a positive influence on the efficiency of the process by using IOF at around 35.7%, which also improved the economy annually. Technically, operating the system with IOF offers positive improvement for dehydration process. However, the trend cannot be generalized since many factors involved in dehydration, particularly water diffusivity and interaction, vary from one product to another [21].

Adjusting the drying operation becomes mandatory to maximize the product quality and amount of energy consumed to achieve the target. COF causes continuous dehydration and exposes the product to heat (for thermal dehydration). Nevertheless, water diffusion requires time to move from internal structure to the surface of product [22]. IOF provides additional relaxation time for the product when the fan shuts off, allowing the product to cool down and accelerating water diffusion to reach moisture equalization [23]. Modification of intermittency cycle is also done for osmotic dehydration and demonstrates various effects [24]. The work [25] gave specific examples for the dehydration of olive using various scenarios (freezing, oven and infrared drying), indicating a certain condition to achieve optimum output for IOF, which depends on the method and processed product. It represents the complexity of dehydration process, which varies from case to case, affected by type of product and chosen method, resulting in different dehydration behavior and quality.

The previous research focused on improving the operation of CGD, showing a serious effort to maximize the applicability of the technology for dehydration process. The efforts mainly focused on enhancing solar radiation input to the system under on-solar duration. Nevertheless, weather is unpredictable, and seasonal changes require additional consideration for the sustainability and continuous dehydration process [26]. Also, limited land available in certain regions comes as another challenge, which makes the processed product need to be arranged specifically, including another technical issue such as shading, which limits the effective daily radiation to CGD [27]. Another factor of the processed product (seaweed) is that it has high moisture content (MC) with strong water molecular force to the structure, which demands a longer dehydration duration [28]. Thus, pre-dehydration can be offered to reduce the given issue, which can be performed under off-solar duration (OSD). It makes further work still required to assess the operation of the system under OSD, offering additional information to maximize the pre-dehydration stage with no solar intensity condition, which is also applicable for seasonal changes such as rain season. It is taken to support and promote a better dehydration cycle under conditions with no solar supply and solely depends on air transfer within the system.

2 MATERIALS AND METHOD

We focused the assessment and evaluation for practical application, hoping the findings is applicable for actual implementation and deliver great impact for society. Thus, the basic model of CGD was designed as even span model considering its common model in the field, which has the most optimum solar radiation input annually [29]. The model schematic is presented in Fig. 1a, including the plan dimension and arrangement of the system assembly. The wall was covered with thin plastic (0.2 mm) UV-HDPE to meet the criteria for on-solar duration at midday [30]. The load (seaweed) was hung inside the CGD and positioned at the center point between intake/exhaust lines. The frame was made from hardwood, while the cladding was attached evenly at the frame to ensure well air circulation from outside to the dehydrator chamber. The system was equipped with twin electric fan (DC) at the exhaust port to force air circulation from the outside to pass the load inside the CGD. The given concept is the most common model of basic operation for CGD and highly relevant to typical actual system. Thus, there is strong correlation between the proposed model and the actual design, making the result from this study applicable to the typical CGD system.

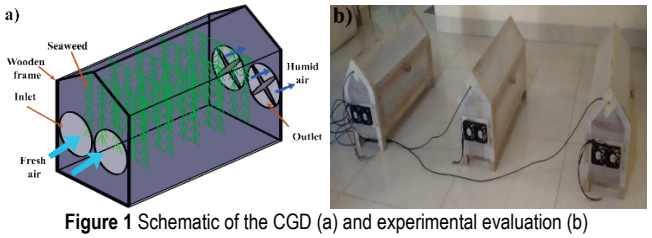


Figure 1 Schematic of the CGD (a) and experimental evaluation (b)

The key parameter for the evaluation is defined according to the mass of the product. It is the most essential point for dehydration process. The initial weight of the load was 0.5 kg (± 4.2%), and it was weighed every hour during the test. The water content (MC) was found at 85% (wet base), showing the typical high MC of aquaculture product. The effective energy is obtained based on the total removed MC from the load. Fig. 1b shows the experimentation unit. It was performed simultaneously for three different parameters. The base variation for evaluation was intake volumetric air flowrate (VAF, $\times 10^{-2}$ m^3/s) which was set at 1.4 (LVAF), 2.2 (MVAF), and 3.1 (HVAF). The fan operation was adjusted based on COF, IOF0.5 (IOF-I) and IOF0.25 (IOF-II). The subscript indicates the cycle schedule of the fan, which was every 30 minutes (IOF-I) and every 15 minutes (IOF-II). For actual comparison, the load was also placed at the outside to determine the baseline of OSD operation without using CGD. The assessment was performed for 10 hours from 07 pm to 05 am (local time) and simultaneously recorded for the RH/T of air inside the CGD and at the ambient.

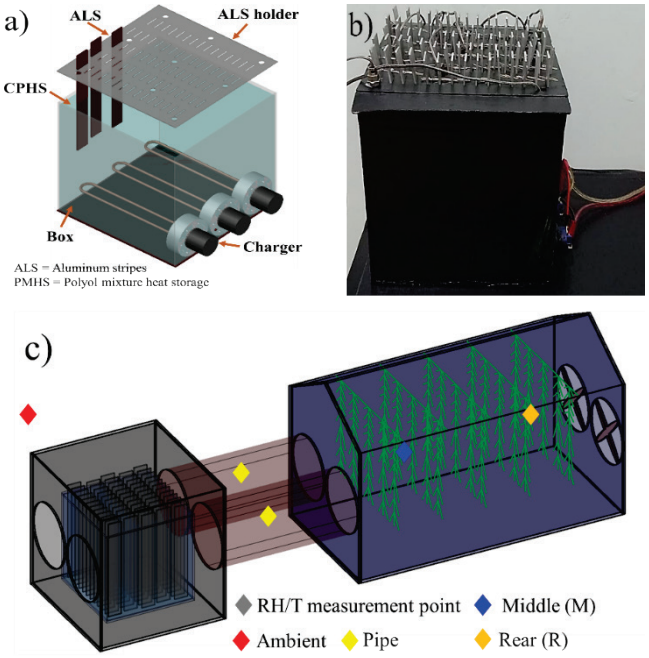


Figure 2 Detail design of thermal box (TBX) (a), its photograph (b) and assembly of system TBX-CGD (c)

The next stage evaluation was conducted according to the best VAF for the system and combined with thermal box (TBX). The TBX is a device that stored thermal energy which commonly absorbs excess heat from sun during optimum solar duration [31–33]. Thus, CGD can be operated by absorbing the stored heat for OSD operation from TBX when its fully charged. The work employed CPHS as material TBX which was made of sorbitol (75%) and mannitol (25%). The polyols offer higher storage density and can operate at elevated temperature, which is suitable for pre-dehydration stage for CGD under OSD operation. Fig. 2a shows the designed TBX for this work. In brief, the model operates using thermal charger from electric power to heat the M-TBX until it reach the designed working temperature. ALS helps accelerate the charge stage by distributing heat properly as the charge process is taken at the lower zone of the assembly. The stored heat was distributed through the body of TBX and the tip of ALS, which directly interacted with the working air before entering CGD. Thus, compact and robust TBX model is obtained, which can be easily developed and implemented for OSD. Fig. 2b presents the photograph of the TBX unit.

The system was evaluated with TBX based on the scheme in Fig. 2c. The fully charged TBX (at 120 °C) was discharged to the OSD through air based on the fan operating scenario. The psychrometric profile for the air was measured at four different regions. The gravimetric capacity of the load was kept the same (0.5 kg). The process provided additional indication of the impact of employing thermal backup based on the designed operation condition for dehydration inside the CGD. Thus, the work assessed two essential OSD operation models, with and without thermal backup, which makes clear interpretation from each operation can be provided to justify the practical condition of CGD operation under OSD.

3 RESULTS AND DISCUSSION

The cyclic operation pattern from the evaluation is observed according to the change of air properties, in this case RH. The pattern is observed since the data was taken every 5 seconds. The obtained data is presented as an arbitrary unit graph (Fig. 3) to maximize the observation of cyclic patterns. The profile demonstrates a clear cyclic pattern as well as the effect of VAF from the process. Under LVAF operation (Fig. 3a), the RH changes inconsistently for the IOF-I and IOF-II. The vast initial water content followed by low VAF results in steep fluctuation of RH value due to high absorption of water molecule by the air. COF shows opposite profile from ambient, which signifies the continuous air evacuation process. It was raining outside the building during the evaluation, which caused the RH ambient to drop dramatically. It is affected by the movement of moist air in the atmosphere, causing the ambient humidity to decrease [34]. The changing pattern for IOF operation demonstrates delayed profile once the fan shuts off, causing the RH to increase slightly before reaching the maximum point when fan sets on.

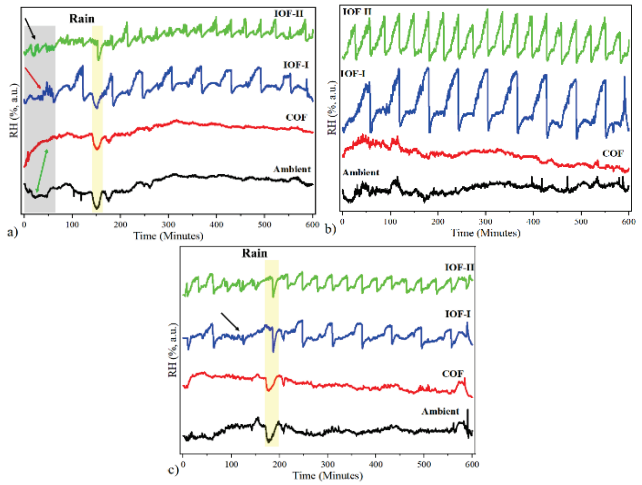


Figure 3 Variation of RH (%) at LVAF (a), MVAF (b) and HVAF (c)

The evaluation of MVAF was conducted on clear night without rain outside the building. Interestingly, the delayed RH profile becomes more apparent at the transition fan operation for IOF-II (Fig. 3b). Higher VAF probably improves the average evacuation rate of moist air, making a higher RH gradient seen distinctly. However, adjusting suitable VAF relative to the volume of CGD is important to consider since the RH value becomes lower at the active cycle (Fig. 3c). Suitable cyclic pattern for MVAF indicates steady operation on the exchange process between the air and water removal from the product. The presence of resting time causes various diffusion process throughout the structure body of the product. Increasing the air velocity may result in slower evaporation, as observed with insignificant RH increment at the initial phase of HVAF operation (black arrow Fig. 3c). The cyclic pattern tends to occur after certain period, showing the time as essential variable for evaporation process of water content from the product. The arbitrary graph allows for a better observation to analyze the impact of each evaluated parameter of the assessment process.

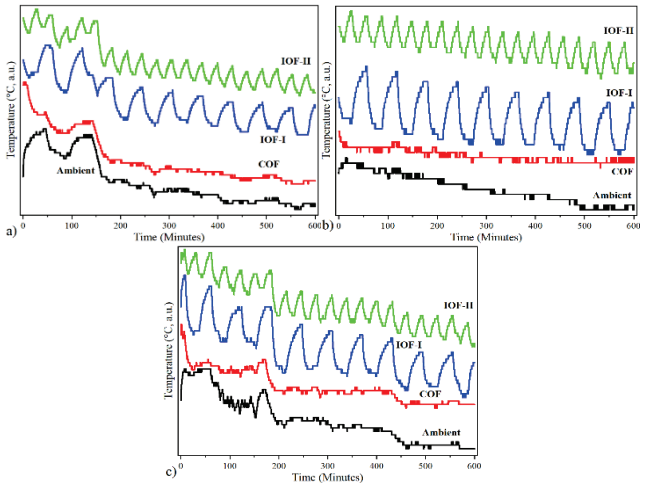


Figure 4 Variation of T (°C) at LVAF (a), MVAF (b) and HVAF (c)

Another psychrometric aspect of air (T, °C) is plotted in Fig. 4. The profile has identical pattern where it tends to decrease as the process continues throughout the night. It implies that evaporative cooling [35] takes place inside the dehydrator. It proves the water removal process from the product to the air. The impact of cyclic process is observed based on T indicator of the process, which is less observed for LVAF operation (Fig. 4a). In contrast, operating the system at MVAF allows to achieve of stationary temperature between active-resting period (Fig. 4b). It causes low-temperature decrement which observed insignificantly between each period. The HVAF operation indicates partial decrement on T at the transition active-resting period (Fig. 4c). It implies the zone experiences further evaporation under free convection mode. It emphasizes there is strong factor which comes from the processed product regarding the water movement inside the cellular structure of product, resulting in different evaporation behavior inside the CGD, particularly under operating without thermal source such as in OSD.

Fig. 5 summarizes the psychrometric value from the evaluation. The presented scale clearly represents the changes in psychrometric aspect (RH/T) throughout the process under different fan operations and speeds. The ambient RH is generally lower than inside the CGD, allowing for possible evaporation process inside CGD under OSD (Fig. 5a). It is justified based on the tendency of higher RH value inside CGD demonstrating water liberation from product to the working fluid, which causes the air becomes more humid. One interesting result is shown for IOF-I profile, which increases by 87.1% (LVAF) and triple times for MVAF. It decreases once the system operates under HVAF. Accordingly, intermittency operation and volumetric speed strongly correlate with the changes in RH value. Moreover, shorter cyclic with IOF-II causes the RH limit to becomes lower than IOF-I and COF (only for HVAF). The changes in RH are simultaneously followed by temperature drop inside CGD (Fig. 5b). However, the temperature variation for all process with different parameter demonstrate identic value, ranging between 0.7 – 3.4 °C. The insignificant temperature variation shows the technical limitation for operating dehydration under OSD, which limits the evaporation cooling rate based on the designed dimension and VAF.

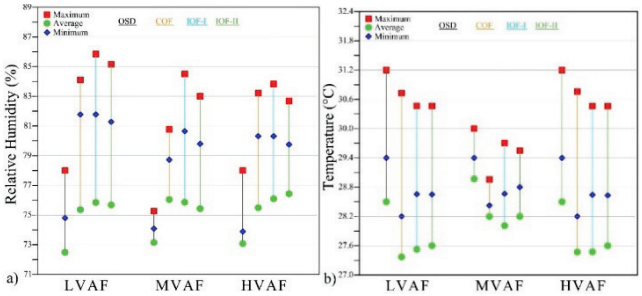


Figure 5 Scaling the RH-T variation of the operation: a) RH map and b) T Map

The changes in RH/T inside CGD indicate the water liberation from product, causing the product mass to decrease along the process. The total mass loss is presented in Fig. 6a and taken as key parameter to compare each evaluation scenario. At this point, locating the product outside (defined as OSD) still causes dehydration since there is air movement due to wind (even though insignificantly), variation of RH and T of the ambient air, and method to place the product (hanging) which increases the contact area with air and accelerate gravitational effect. Unfortunately, it results in insignificant dehydration rate since the process occurs as free convection without involving any thermal source. In contrast, employing fan to accommodate force convection inside CGD contributes to the higher total mass loss. It is also observed that increasing the VAF and continue operation yield higher total mass loss around 47.3%. The impact of changing the intermittency is observed distinctly as the VAF increases, indicating that evaporation can be accelerated as the average mass transfer improves within the system.

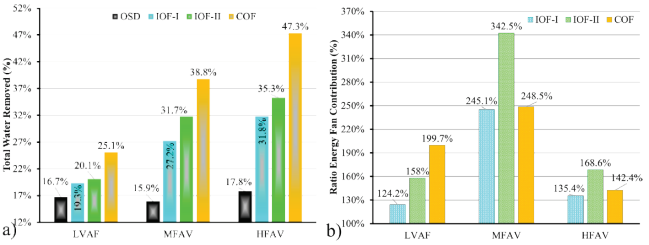


Figure 6 Total mass loss (a) and ratio useful energy from fan (b)

The primary goal for operating the system at OSD is pre-dehydration stage, making the consumed energy the most crucial factor to consider. Each process (Fig. 6b) shows different results, which implies that additional points need to be considered regarding the effectiveness of OSD operations. The amount of liberated water from product under CGD operation is subtracted by total water removal from OSD (baseline). The net liberated water is multiplied by standard latent heat of vaporization and compared by the energy consumed by the component (fans). It is plotted as ratio of energy fan contribution. As observed, it has positive value (higher than 100%), which indicates that the total water removed is higher than energy consumed by the fan.

The LVAF requires suitable fan operating, resulting in higher energy effectiveness for continuous cycle and shorter intermittency. However, dehydration takes time for the water molecule to diffuse throughout the product, making continuity and increasing the fan speed not always proportional in terms of effective energy consumption. It is shown notably for the MVAF, where IOF-I (30 minutes intermittency) and COF (continue) have identic ratio. In contrast, IOF-II (15 minutes intermittency) allows the system to achieve the highest effectiveness from the energy input to operate fans. Increasing the operation speed (HVAF) decreases the effective energy input since the fan consumes more energy. The major finding of this work is that operational parameters are essential for optimum OSD operation and can be modified according to the system and product conditions to achieve the highest effective energy ratio throughout the process.

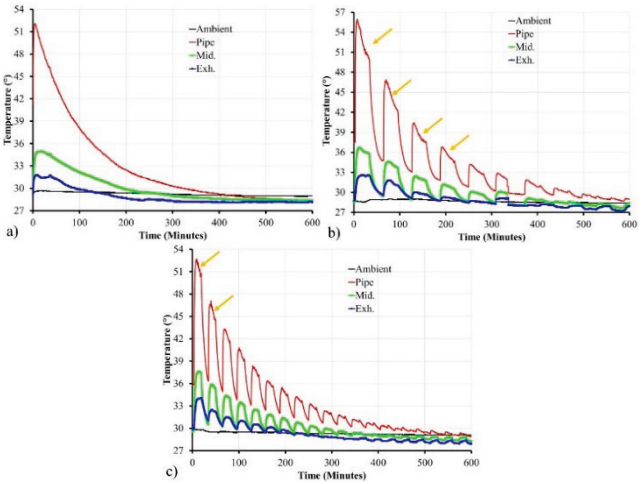


Figure 7 Changing of temperature of the assembly TBX-CGD for a) COF, b) IOF-I, and c) IOF-II

The system is tested by combining TBX as thermal backup for CGD under speed MVAF. The observed RH/T value for each location of the assembly (Fig. 2c) is presented in Fig. 7. All zone shows indications for temperature increment as a result of the addition TBX, where the value becomes lower as the measurement farther from the heat source. The effect of operation setting for the CGD changes the temperature pattern. For example, COF shows consistent temperature decrement from the pipe to the inside CGD (Fig. 7a). The temperature initially increases by 75.4% at the pipe zone and steadily decreases to 7% at the exhaust region. The TBX has a finite capacity, making the effective operation only 400 minutes according to the plotted temperature.

Fig. 7b presents the cyclic pattern of IOF-I, allowing the discharge stage to be extended until the final evaluation. It achieves a higher increment on the temperature at 93.1%, with the lowest point at 12.4%. A short delay region (brown arrow) for the discharged heat indicates that TBX takes time to perform heat exchange with air. It is probably advantageous for dehydration to prevent the product from overheating due to sudden high-temperature exposure. Shorter-cyclic (IOF-II, Fig. 7c) shows a relatively similar pattern with IOF-II. Even though the maximum increment is lesser than IOF-II (only 76.3%), the exhaust zone temperature maintained a higher value at 34.1 °C.

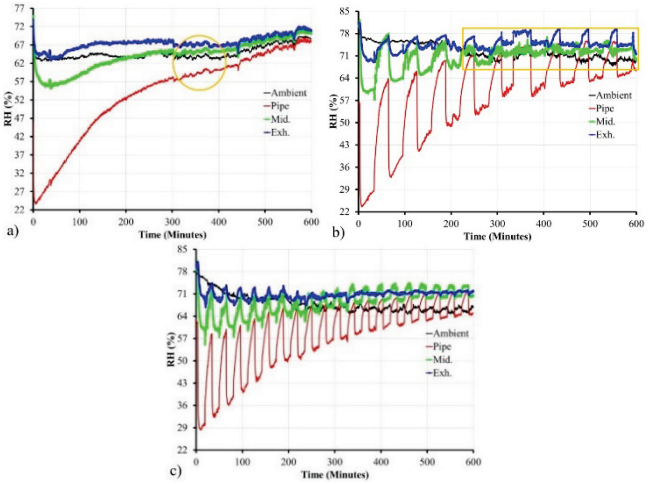


Figure 8 Changing of RH of the assembly TBX-CGD for a) COF, b) IOF-I, and c) IOF-II

TBX transfers heat to the air, causing it to expand and resulting in a lower RH. As the cycle continues and the heat diminishes (brown circle Fig. 8a), the air contracts, leading to a higher RH inside CGD. In contrast with T, RH changes rapidly as the system operates, causing overlap phenomenon and constantly changing the RH value relatively at higher/lower conditions than the ambient. IOF-I shows this condition notably (brown rectangular Fig. 8b), while IOF-II indicates a lower cyclic effect regarding the interlapping RH value (Fig. 8c).

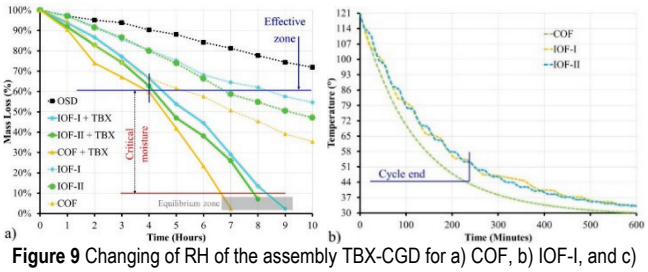


Figure 9 Changing of RH of the assembly TBX-CGD for a) COF, b) IOF-I, and c) IOF-II

The role of dehydration is presented as the decrement of mass of the product. It is plotted in Fig. 9a for the system with and without TBX for a clearer evaluation. The mass decreases higher for COF and IOF-II, indicating the key role of forced air transfer in performing dehydration at night-time. Adding thermal backup, in this case TBX, accelerates the evaporation, eventually increasing the mass loss to achieve the equilibrium moisture. However, the presence of TBX is not intended to perform direct drying to achieve equilibrium moisture due to disproportional pair-to-pair gravimetry capacity from the TBX and the load. For illustration, the MTBX was 10 kg while the load was merely 0.5 kg. It is totally imbalanced from a practical perspective since the storage has more capacity than the designed load. The key role of TBX is essential to achieve critical moisture, which occurs at mass 60-70%. One undeniable proof is that all

operations show the same duration to achieve critical moisture, indicating that the TBX is more advantageous in accelerating the initial dehydration phase. Moreover, the temperature inside TBX remains higher at capacity of 15% (according to minimum/maximum temperature deviation inside the TBX) when it comes to the end of cycle of pre-dehydration stage (Fig. 9b). It is favorable for TBX since it reduces initial charge stage which typically requires more energy under solid-sensible stage of the material inside TBX.

4 CONCLUSION

The work shows high feasibility and opportunity to utilize OSD to perform pre-dehydration stage, which probably increases the batch capacity per day and prevents severe loss during low-intensity solar season. Technical barrier such as low dehydration performance is solved by adjusting the system to operate sufficiently, reducing the net energy consumption while maintaining the reasonable total water removed. Indeed, operating the fan at higher evacuation rate with continuous active cycle results in the maximum total dehydration. Unfortunately, this act has low positive energy coefficient, which is merely 142.4%. Also, operating the system with a relatively long cyclic setting causes an extended tempering period, reducing the maximum water removed from product. At this point, shorter cyclic with suitable evacuation rate contributes to a positive achievement in terms of effective energy ratio for operating fan, which increased to 342.5%. The absence of heat input for OSD is solved by using thermal backup, allowing the system to reach the critical moisture faster. It is found that all scenarios show identic duration for the product to reach critical moisture level. Operating the backup heating energy under suitable control allows the system to achieve effectivity level of 22.7%. One critical finding shows that forcing the system to achieve equilibrium moisture (dry) is technically inefficient, reaching maximum point effectivity level at 9.3%.

Overall, the finding reveals that OSD is applicable to support the development and capacity of typical solar drying. It is only achieved by adjusting the system to operate with suitable cyclic duration and evacuation rate, even though the MC of product is considerably high (above 80%). This initial evaluation promotes OSD for optimizing the drying process, making additional work advisable to achieve a higher technology output. It is important to conduct continuous cycle from effective solar duration and assess the entire energy consumption of the process, including critical factors involving the operation and feasibility, such as techno-economy evaluation. We believe the finding from this work, which can be further improved, offers a clear breakthrough to encourage the development of clean food production, supporting responsible consumption and enhancing the affordable clean energy goal as part of community service from researcher and industrialist.

5 REFERENCES

[1] Vallejo-Díaz, A., Herrera-Moya, I., Fernández-Bonilla, A., & Pereyra-Mariñez, C. (2022). Wind energy potential assessment of selected locations at two major cities in the Dominican Republic, toward energy matrix decarbonization, with resilience approach. *Thermal Science and Engineering Progress, 32*, 101313. https://doi.org/10.1016/j.tsep.2022.101313

[2] Lahnaoui, A., Aniello, G., Barberis, S., Nwabueze Agbo, S., & Kuckshinrichs, W. (2024). Assessing the feasibility of a green hydrogen economy in selected African regions with composite indicators. *International Journal of Hydrogen Energy, 101*, 1387-1405. https://doi.org/10.1016/j.ijhydene.2024.12.233

[3] Assareh, E., Agarwal, N., Paul, M. C., Ahmadi, P., Ghodrat, M., & Lee, M. (2023). Investigation and development of a novel solar-biomass integrated energy system for clean electricity and liquid hydrogen production. *Thermal Science and Engineering Progress, 42*, 101925. https://doi.org/10.1016/j.tsep.2023.101925

[4] Wang, J., Kong, Y., Liu, Z., & Wang, H. (2023). Solar-driven interfacial evaporation: Design and application progress of structural evaporators and functional distillers. *Nano Energy, 108*, 108115. https://doi.org/10.1016/j.nanoen.2022.108115

[5] Muflikh, Y. N., Permani, R., Nuryartono, N., Pasaribu, S. H., Julianto, B. S., Sjahruddin, F., et al. (2024). Building stakeholders' mutual understanding of seaweed sustainability in Indonesia: A group model building approach. *Marine Policy, 168*, 106283. https://doi.org/10.1016/j.marpol.2024.106283

[6] Chaatouf, D., Raillani, B., Salhi, M., Amraqui, S., & Mezrhab, A. (2023). Experimental and numerical study of a natural convection indirect solar dryer with PCM tubes: Dynamic, thermal and nutritional quality analysis. *Solar Energy, 264*, 111975. https://doi.org/10.1016/j.solener.2023.111975

[7] Demissie, Y. A., Abreham, R. E., Wassie, H. M., & Getie, M. Z. (2024). Advancements in solar greenhouse dryers for crop drying. *Energy Reports, 11*, 5046-5058. https://doi.org/10.1016/j.egyr.2024.04.058

[8] Atalay, H., & Aslan, V. (2023). Advanced exergoeconomic and exergy performance assessments of a wind and solar energy powered hybrid dryer. *Renewable Energy, 209*, 218-230. https://doi.org/10.1016/j.renene.2023.03.137

[9] Atalay, H., Yavaş, N., & Turhan Çoban, M. (2022). Sustainability and performance analysis of a solar and wind energy assisted hybrid dryer. *Renewable Energy, 187*, 1173-1183. https://doi.org/10.1016/j.renene.2022.02.020

[10] Khalil, A., Khaira, A. M., Abu-Shanab, R. H., & Abdelgaied, M. (2023). A comprehensive review of advanced hybrid technologies that improve the performance of solar dryers: Photovoltaic/thermal panels, solar collectors, energy storage materials, biomass, and desalination units. *Solar Energy, 253*, 154-174. https://doi.org/10.1016/j.solener.2023.02.032

[11] Tiwari, A., & Kumar, A. (2023). Solar air heater based on double-ends open evacuated tube with and without phase change material: An experimental investigation. J*ournal of Energy Storage, 72*, 108265. https://doi.org/10.1016/j.est.2023.108265

[12] Anish, R., Mariappan, V., Joybari, M. M., & Abdulateef, A. M. (2020). Performance comparison of the thermal behavior of xylitol and erythritol in a double spiral coil latent heat storage system. *Thermal Science and Engineering Progress, 15*, 100441. https://doi.org/10.1016/j.tsep.2019.100441

[13] Rahman, R. A., Sulistyo, S., Utomo, M. S. K. T. S., & Dhewangga Putra, R. D. (2024). The optional approach in recycling plastic waste for energy storage application: A detailed evaluation of stabilized–hexadecanoic acid/plastic. *Case Studies in Chemical and Environmental Engineering, 9*, 0-5. https://doi.org/10.1016/j.cscee.2024.100751

[14] Murugesan, G. K., Murugesan, C., Sakthivel, M., & Tamilkolundu, S. (2024). Experimental investigation on a solar dryer assisted with minimum phase change material (PCM) placed on the inner walls of drying chamber. *Journal of Energy Storage, 98*. https://doi.org/10.1016/j.est.2024.113069

[15] Palacio, M., Ramírez, C., Carmona, M., & Cortés, C. (2022). Effect of phase-change materials in the performance of a solar air heater. *Solar Energy, 247*, 385-396. https://doi.org/10.1016/j.solener.2022.10.046

[16] Khanlari, A., Sözen, A., Şirin, C., Tuncer, A. D., & Gungor, A. (2020). Performance enhancement of a greenhouse dryer: Analysis of a cost-effective alternative solar air heater. *Journal of Cleaner Production, 251*. https://doi.org/10.1016/j.jclepro.2019.119672

[17] Carlos, J., Pereira, A., Pereira, W., Gomes, J. P., Jos, A., Melo, D., et al. (2020). Continuous and intermittent drying of rough rice: Effects on process effective time and effective mass diffusivity. *Agriculture (Switzerland), 10*, 0-5.

[18] Li, M., Geng, Z., Zhang, X., Yang, X., & Zhang, Q. (2025). Establishment and application of a simulation model for infrared radiation combined with hot air intermittent drying of jujube slices. *LWT, 215*, 117280. https://doi.org/10.1016/j.lwt.2024.117280

[19] Hou, Y., Wu, W., Wang, H., Zhang, H., & Guan, C. (2025). Effect of intermittent ratio on the performance of a closed-loop heat pump drying system with a novel ternary refrigerant and on the drying characteristics of corn kernels. *International Communications in Heat and Mass Transfer, 161*, 108541. https://doi.org/10.1016/j.icheatmasstransfer.2024.108541

[20] Hadibi, T., Mengjie, S., Jiangtao, R., Wang, Y., Benseddik, A., Ming, L., et al. (2025). Comprehensive analysis and experimental study on the novel intermittent solar-electric onion drying technology. *Renewable Energy, 238*, 121949. https://doi.org/10.1016/j.renene.2024.121949

[21] Van Engeland, C., Spreutels, L., Legros, R., & Haut, B. (2022). Comprehensive analysis of intermittent drying: A theoretical approach. *Food and Bioproducts Processing, 131*, 86-101. https://doi.org/10.1016/j.fbp.2021.10.009

[22] González-Pérez, J. E., Romo-Hernández, A., López-Malo, A., & Ramírez-Corona, N. (2023). Evaluation of osmodehydration and vacuum-assisted osmodehydration as pre-treatments during fruit drying process: The effect on drying rates, effective water diffusion and changes in product quality. *Journal of Engineering Research (Kuwait), 11*, 275-282. https://doi.org/10.1016/j.jer.2023.100153

[23] Bissaro, C. A., de Souza Matias, G., Defendi, R. O., & de Matos Jorge, L. M. (2022). Modeling the drying kinetics of soybeans under intermittent operation in thin layer. *Food and Bioproducts Processing, 136*, 226-235. https://doi.org/10.1016/j.fbp.2022.10.006

[24] Tsopwo Zena, C., & Jiokap Nono, Y. (2024). Investigating intermittent immersion during osmotic dehydration of mango (Mangifera indica L. Moench). Part A: Determination of optimal conditions for mango (Mangifera indica L. Moench) dehydration impregnation by immersion (D2I) and intermittent immersion. *Heliyon, 10*, e39389. https://doi.org/10.1016/j.heliyon.2024.e35808

[25] Pyrka, I., Mantzouridou, F. T., & Nenadis, N. (2023). Optimization of olive leaves' thin layer, intermittent near-infrared drying. *Innovative Food Science and Emerging Technologies, 84*, 103264. https://doi.org/10.1016/j.ifset.2022.103264

[26] Pandey, S., Kumar, A., & Sharma, A. (2024). Sustainable solar drying: Recent advances in materials, innovative designs, mathematical modeling, and energy storage solutions. *Energy, 308*, 132725. https://doi.org/10.1016/j.energy.2024.132725

[27] Chong, S., You, J., Wu, J., & Chang, I. S. (2024). Booming solar energy drives land value enhancement: Evidence from 648 photovoltaic projects in China. *Journal of Cleaner Production, 484*, 144270. https://doi.org/10.1016/j.jclepro.2024.144270

[28] Amir, N., Imron Mustajib, M., Gozan, M., & Chan, C. (2024). Development of a novel tray solar dryer for aquaculture product: Experimental study on drying kinetics and product quality in Eucheuma cottonii seaweed. *Solar Energy, 273*, 112503. https://doi.org/10.1016/j.solener.2024.112503

[29] Paing, S. T., & Anderson, T. N. (2024). Characterizing the effects of geometry on the natural convection heat transfer in closed even-span gable-roof greenhouses. *Thermal Science and Engineering Progress, 48*, 102408. https://doi.org/10.1016/j.tsep.2024.102408

[30] Srinivasan, G., & Muthukumar, P. (2021). A review on solar greenhouse dryer: Design, thermal modelling, energy, economic and environmental aspects. *Solar Energy, 229*, 3-21. https://doi.org/10.1016/j.solener.2021.04.058

[31] Ranjan Tamuli, B., & Nath, S. (2023). Analysis of micro heat pipe array based evacuated tube solar water heater integrated with an energy storage system for improved thermal performance. *Thermal Science and Engineering Progress, 41*, 101801. https://doi.org/10.1016/j.tsep.2023.101801

[32] Rahman, R. A., Sulistyo, S., Utomo, M. S. K. T. S., Ragil, D., & Suyitno, B. M. (2024). Experimental evaluation on the power characteristic of direct-photovoltaic charging for thermal storage equipment. *Mechanical Engineering for Society and Industry, 4*, 115-122.

[33] NematpourKeshteli, A., Iasiello, M., Langella, G., & Bianco, N. (2024). Using metal foam and nanoparticle additives with different fin shapes for PCM-based thermal storage in flat plate solar collectors. *Thermal Science and Engineering Progress, 52*, 102690. https://doi.org/10.1016/j.tsep.2024.102690

[34] Acero, J. A., Kestel, P., Dang, H. T., & Norford, L. K. (2024). Impact of rainfall on air temperature, humidity, and thermal comfort in tropical urban parks. *Urban Climate, 56*, 102051. https://doi.org/10.1016/j.uclim.2024.102051

[35] Lv, G., Ji, X., Yang, B., Chen, Y., & Xu, H. (2024). Operating modes study of evaporative cooling-dehumidification air conditioning under different climatic conditions. *Applied Thermal Engineering, 243*, 122597. https://doi.org/10.1016/j.applthermaleng.2024.122597

Authors' contacts:

Nursiwan, Master Student
Department of Mechanical Engineering,
Faculty of Engineering, Universitas Pancasila,
Srengseng Sawah, Jagakarsa 12640, DKI Jakarta, Indonesia
E-mail: nursiwanalif@yahoo.com

Samsul Arifin, Master Student
Department of Mechanical Engineering,
Faculty of Engineering, Universitas Pancasila,
Srengseng Sawah, Jagakarsa 12640, DKI Jakarta, Indonesia
E-mail: abngsamsul1400@gmail.com

Budhi Muliawan Suyitno, Full professor, Dr.
Department of Mechanical Engineering,
Faculty of Engineering, Universitas Pancasila,
Srengseng Sawah, Jagakarsa 12640, DKI Jakarta, Indonesia
E-mail: budhi.suyitno@univpancasila.ac.id

Reza Abdu Rahman, Assistant Professor, Dr.
(Corresponding author)
Department of Mechanical Engineering,
Faculty of Engineering, Universitas Pancasila,
Srengseng Sawah, Jagakarsa 12640, DKI Jakarta, Indonesia
E-mail: reza.a@univpancasila.ac.id